

## A Simple and Convenient Method to Fabricate Hexagonally Ordered Gold Nanoparticle Arrays Using Diblock Copolymer Micelle Template

Shigeru Watanabe,<sup>\*1</sup> Shin Nakano,<sup>1</sup> Chie Imai, Inamur R. Laskar,<sup>1,†</sup>  
Tomonori Komura,<sup>2</sup> Shingo Hadano,<sup>2</sup> and Tomokazu Iyoda<sup>2</sup>

<sup>1</sup>Department of Applied Science, Faculty of Science, Kochi University, 1-2-5 Akebono-cho, Kochi 780-8520

<sup>2</sup>Chemical Resource Laboratory, Tokyo Institute of Technology,  
1-25-4259 Nagatsuda, Midori-ku, Yokohama, Kanagawa 226-8503

(Received May 24, 2010; CL-100496; E-mail: watanabe@kochi-u.ac.jp)

Monolayer films of hexagonally ordered diblock copolymer micelles were prepared as templates by self-assembly. Gold nanoparticles immediately self-assembled on each individual micelle upon immersion of the template in an aqueous solution of the nanoparticles. This provided a simple, convenient, and inexpensive nanofabrication technique for manufacturing ordered arrays of gold nanoparticles over an extended area.

There has been an enormous effort to achieve controllable fabrication of metal nanoparticles due to their potential applications in a variety of areas, such as catalysis, sensors, electronics, optics, and magnetics.<sup>1–4</sup> One of the most promising approaches for patterning nanoparticles is to use self-assembled nanostructures of block copolymers as templates.<sup>5,6</sup> Block copolymer micelles (BCMs) have been used as nanotemplates and nanomasks to assemble and pattern nanostructures.<sup>7–18</sup> There are two main approaches to fabricating nanoparticles using BCMs as templates.<sup>8c</sup> In the first approach, BCMs are loaded onto a substrate to form a self-assembled monolayer, after which the substrate and monolayer are immersed in a solution of metal salts, which serve as precursors to the desired nanoparticles. Arrays of nanoparticles can then be prepared in situ on the substrate by subsequent plasma etching to remove the polymer material and convert the precursors in the micelle cores to nanoparticles. In the second approach, BCMs carrying the metallic precursor are loaded onto a substrate and subjected to plasma etching. However, these techniques are generally limited to the fabrication of small nanoparticles and are not suitable for applications requiring larger nanoparticles, such as local surface plasmon resonance (LSPR) and surface-enhanced resonance scattering (SERS) sensors. To control nanoparticle size, electroless deposition is usually necessary, which increases the complexity of the process.<sup>7a</sup> Further improvement of these complex and multistep processes is, therefore, required. Here we report a very effective and simple method for fabricating hexagonally ordered arrays of relatively large AuNPs ( $d > 10$  nm) using a BCM template (Figure 1).

Well-ordered monolayer films of BCMs were prepared by self-assembly of a block copolymer followed by solvent annealing.<sup>9a</sup> A 0.5 wt % solution of polystyrene-*block*-poly(4-vinylpyridine) (PS-*b*-P4VP) ( $M_n^{\text{PS}} = 50000 \text{ g mol}^{-1}$ ,  $M_n^{\text{P4VP}} = 13000 \text{ g mol}^{-1}$ , polydispersity index 1.04, Polymer Source, Inc.) in toluene was stirred for 72 h to assemble into spherical micelles with a PS corona and a P4VP core. A single layer of PS-*b*-P4VP was then formed by spin-coating the toluene solution onto cleaned glass substrates at 2000 rpm. To construct hexagonally ordered defects in these films, the as-prepared

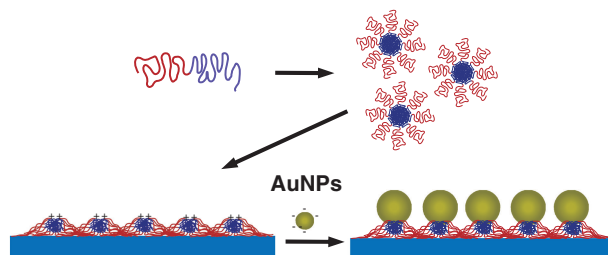


**Figure 1.** Schematic of the process for block copolymer micelle templated nanopatterning of metal nanoparticles.

micelle monolayer was solvent-annealed in saturated THF vapor at 40 °C for 2 h.

The annealed films were immersed in a solution of citrate-stabilized AuNPs<sup>19</sup> ( $d = 13.6 \pm 1.2$  nm) for various periods of time. AFM images taken after immersion showed that the height of the BCMs increased by  $7.01 \pm 0.51$  nm, indicating that the AuNPs were placed on each of the PS-*b*-P4VP micelles (Figure 2). Core–corona inversion is induced when a monolayer film of PS-*b*-P4VP micelles is exposed to a selective solvent for the P4VP core.<sup>9b,12b</sup> Consequently, self-assembly of negatively charged AuNPs onto the BCMs could be driven by electrostatic binding of the nanoparticles to the P4VP block positively charged by protonation. The surface coverage of the self-assembled AuNPs increased with immersion time. However, excessively lengthy immersions caused aggregation of the AuNPs, negating the templating effect of the BCMs. After 5 min of immersion, the AuNPs showed almost perfect hexagonal ordering on individual BCMs (Figure 2b). These assemblies were also observed with a field emission scanning electron microscope (FE-SEM, Hitachi S-5200, Japan) at an accelerating voltage of 1 kV, which showed that the hexagonally ordered AuNP arrays covered large (micrometer scale) areas (Figure 3).

Grazing-incidence small-angle X-ray scattering (GISAXS) measurements also supported the above-mentioned claims of two-dimensional hexagonal ordering of the AuNPs. GISAXS experiments were performed on a Nano-Viewer (Rigaku, Japan) equipped with a two-dimensional charge-coupled detector (CCD) using Cu K $\alpha$  radiation ( $\lambda = 1.541 \text{ \AA}$ ) and an incidence angle of 0.21°, close to the critical reflection angle of the amorphous SiO<sub>2</sub> substrate, to effectively obtain in-plane signals. Figure 4a shows the 2D GISAXS pattern exhibiting several strong scattering peaks in the in-plane region near a Yoneda peak.<sup>21</sup> The in-plane intensity profile contains three distinct scattering peaks (Figure 4b). The broad diffraction peak at high  $q$  ( $0.817 \text{ nm}^{-1}$ )

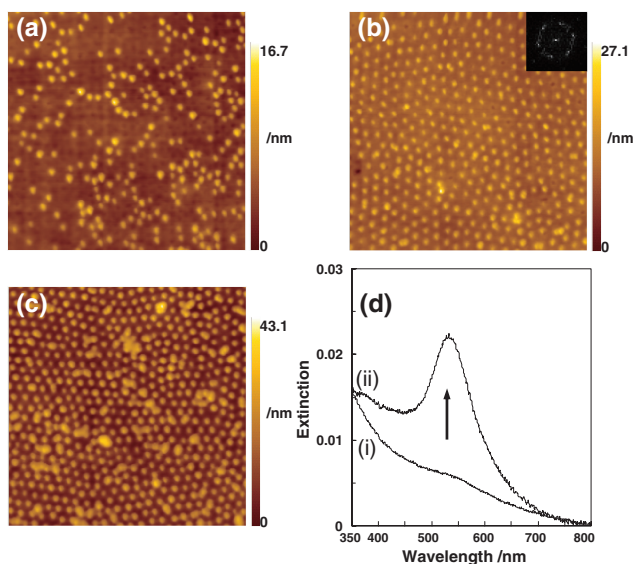


**Figure 2.** AFM topography images ( $1000 \times 1000 \text{ nm}^2$ ) of the THF-annealed monolayer of PS<sub>50000</sub>-*b*-P4VP<sub>13000</sub> micelles after immersion in an aqueous solution of 13-nm AuNPs for various periods of time: (a) 1, (b) 5, and (c) 10 min. (d) UV-vis extinction spectra of the AuNP array prepared by different methods: (i) A glass substrate was coated with a self-assembled monolayer of the BCMs and immersed in aq. HAuCl<sub>4</sub> followed by VUV/O<sub>3</sub> etching (the previously reported method).<sup>20</sup> (ii) A glass substrate was coated with a self-assembled monolayer of the BCMs followed by deposition of gold nanoparticles (the present method).

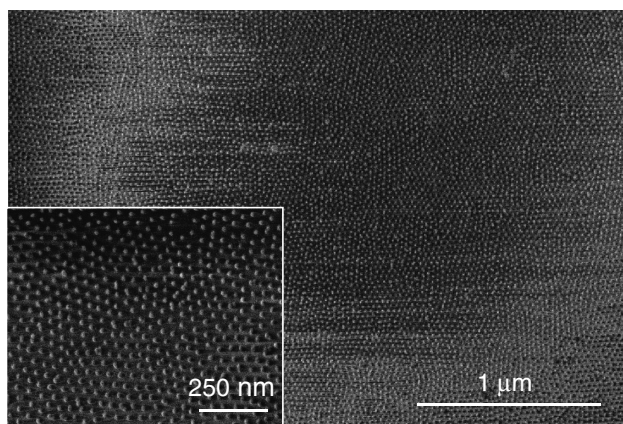


**Figure 3.** FE-SEM images of the self-assembled AuNPs on a PS<sub>50000</sub>-*b*-PMA(Az)<sub>13000</sub> micelle template.

could be attributed to the scattering with size distribution of the AuNPs ( $d = 14.1 \pm 1.5 \text{ nm}$ ), consistent with the value of 13.6 nm measured by TEM. The in-plane diffraction peaks at  $0.171$  and  $0.300 \text{ nm}^{-1}$  corresponded to relative scattering vector lengths from the specular reflection positions of 1 and  $\sqrt{3}$ , respectively. These scattering peaks were characteristic of a 2D hexagonally arranged structure, indicating that the AuNPs were hexagonally packed in a planar monolayer. The average distance between neighboring AuNPs was calculated to be 42.4 nm, consistent with the value of 41.0 nm measured by FE-SEM. It is

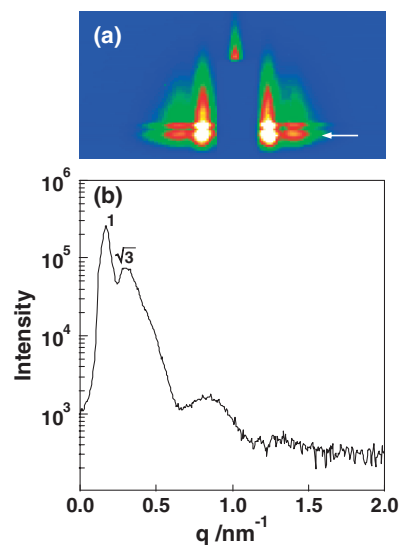


**Figure 4.** (a) 2D GISAXS pattern of the self-assembled gold nanoparticles on a PS<sub>50000</sub>-*b*-PMA(Az)<sub>13000</sub> micelle template. The arrow shows the Yoneda peak arising from the in-plane direction due to the interference of the incident and scattered waves. (b) In-plane intensity profile extracted at the grazing exit angle of  $0.21^\circ$  from the scattering pattern in (a).

noteworthy that the average distance between neighboring AuNPs correlated well with that ( $42.0 \pm 1.1 \text{ nm}$ ) between the neighboring core-corona micelles used as the template.

The arrays prepared by the present method exhibited a distinctive LSPR band at 520 nm (Figure 2d(ii)), while AuNPs prepared by a previously reported method<sup>20</sup> were too small to show this characteristic feature (Figure 2d(i)). In order to evaluate the possible application of these arrays in LSPR sensors, we investigated their optical response to changes in various glycerol solutions having different refractive indices (Figure 5). The UV-vis extinction spectra of the AuNP arrays exhibited an increase in LSPR band intensity along with a slight red shift in the peak wavelength as the refractive index of the solvent increased. The change in the maximum extinction was linear ( $R = 0.986$ ) over the refractive index range studied. From the slope of this plot, the sensitivity factor ( $E_{\text{max}}/\Delta n$ ) was calculated to be  $0.13 \text{ RIU}^{-1}$ . These ordered arrays were sensitive enough to detect molecular recognition phenomena at the surface of the AuNPs.

In conclusion, we have developed the fast, easy, and inexpensive directed self-assembly of AuNPs using a monolayer of PS-*b*-P4VP micelles as a template. The present technique could be used to fabricate hexagonally ordered arrays of relatively large AuNPs over extended areas using few processing steps. Such gold nanostructured films could find use as optical biosensors based on local surface plasmon resonance and are currently under investigation.

This work was financially supported by Grants-in-Aid for Scientific Research from the Ministry of Education, Culture, Sports, Science and Technology, Japan (No. 18101005 and No. 21550084), Japan Society for the Promotion of Science (JSPS), and the Kochi University President's Discretionary Grant.

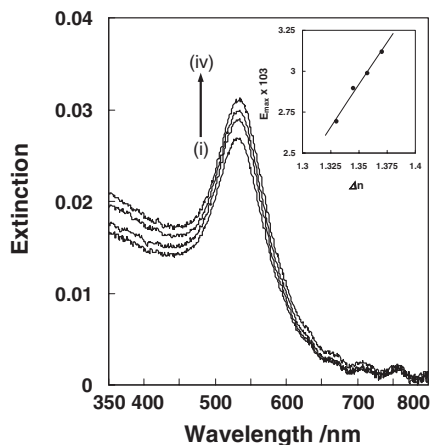


**Figure 5.** Extinction spectra of the self-assembled AuNPs on the BCM template in solvents of different refractive indices. Solvents: (i) water ( $n = 1.33$ ), (ii) 10% glycerol/water ( $n = 1.3448$ ), (iii) 20% glycerol/water ( $n = 1.3572$ ), and (iv) 30% glycerol/water ( $n = 1.3703$ ). The inset is a plot of the maximum extinction ( $E_{\max}$ ) as a function of the refractive index of the surrounding medium.

#### References and Notes

- † Present address: Department of Chemistry, Birla Institute of Technology, Pilani, Rajasthan 333 031, India
- G. A. Somorjai, F. Tao, J. Y. Park, *Top. Catal.* **2008**, *47*, 1.
  - M. De, P. S. Ghosh, V. M. Rotello, *Adv. Mater.* **2008**, *20*, 4225.
  - M. Pelton, J. Aizpurua, G. Bryant, *Laser Photonics Rev.* **2008**, *2*, 136.
  - S. Srivastava, N. A. Kotov, *Soft Matter* **2009**, *5*, 1146.
  - H.-C. Kim, S.-M. Park, W. D. Hinsberg, *Chem. Rev.* **2010**, *110*, 146.
  - J. Bang, U. Jeong, D. Y. Ryu, T. P. Russell, C. J. Hawker, *Adv. Mater.* **2009**, *21*, 4769.
  - a) T. Lohmueller, E. Bock, J. P. Spatz, *Adv. Mater.* **2008**, *20*, 2297. b) G. Kästle, H.-G. Boyen, F. Weigl, G. Lengl, T. Herzog, P. Ziemann, S. Riethmüller, O. Mayer, C. Hartmann, J. P. Spatz, M. Möller, M. Ozawa, F. Banhart, M. G. Garnier, P. Oelhafen, *Adv. Funct. Mater.* **2003**, *13*, 853. c) R. Glass, M. Arnold, J. Blümmel, A. Küller, M. Möller, J. P. Spatz, *Adv. Funct. Mater.* **2003**, *13*, 569. d) M. Haupt, S. Miller, R. Glass, M. Arnold, R. Sauer, K. Thonke, M. Möller, J. P.

- Spatz, *Adv. Mater.* **2003**, *15*, 829.
- a) Y. Qiao, D. Wang, J. M. Buriak, *Nano Lett.* **2007**, *7*, 464. b) M. Aizawa, J. M. Buriak, *Chem. Mater.* **2007**, *19*, 5090. c) M. Aizawa, J. M. Buriak, *J. Am. Chem. Soc.* **2005**, *127*, 8932.
  - a) S.-H. Yun, S. I. Yoo, J. C. Jung, W.-C. Zin, B.-H. Sohn, *Chem. Mater.* **2006**, *18*, 5646. b) B.-H. Sohn, S.-I. Yoo, B.-W. Seo, S.-H. Yun, S.-M. Park, *J. Am. Chem. Soc.* **2001**, *123*, 12734.
  - B.-H. Sohn, J.-M. Choi, S. I. Yoo, S.-H. Yun, W.-C. Zin, J. C. Jung, M. Kanehara, T. Hirata, T. Teranishi, *J. Am. Chem. Soc.* **2003**, *125*, 6368.
  - H. Acharya, J. Sung, B.-H. Sohn, D. H. Kim, K. Tamada, C. Park, *Chem. Mater.* **2009**, *21*, 4248.
  - a) S. Krishnamoorthy, R. Pugin, J. Brugger, H. Heinzelmann, C. Hinderling, *Adv. Mater.* **2008**, *20*, 1962. b) S. Krishnamoorthy, R. Pugin, J. Brugger, H. Heinzelmann, A. C. Hoogerwerf, C. Hinderling, *Langmuir* **2006**, *22*, 3450.
  - M.-V. Meli, R. B. Lennox, *Langmuir* **2003**, *19*, 9097.
  - a) Y. Liu, C. Lor, Q. Fu, D. Pan, D. Lei, J. Liu, J. Lu, *J. Phys. Chem. C* **2010**, *114*, 5767. b) J. Lu, S. S. Yi, T. Kopley, C. Qian, J. Liu, E. Gulari, *J. Phys. Chem. B* **2006**, *110*, 6655.
  - X. Li, K. H. A. Lau, D. H. Kim, W. Knoll, *Langmuir* **2005**, *21*, 5212.
  - H.-G. Boyen, G. Kästle, K. Zürn, T. Herzog, F. Weigl, P. Ziemann, O. Mayer, C. Jerome, M. Möller, J. P. Spatz, M. G. Garnier, P. Oelhafen, *Adv. Funct. Mater.* **2003**, *13*, 359.
  - I. R. Laskar, S. Watanabe, M. Hada, H. Yoshida, J. Li, T. Iyoda, *Surf. Sci.* **2009**, *603*, 625.
  - D. Yin, S. Horiuchi, T. Masuoka, *Chem. Mater.* **2005**, *17*, 463.
  - G. Frens, *Nature (London), Phys. Sci.* **1973**, *241*, 20.
  - Hexagonally ordered arrays of AuNPs were prepared as follows:<sup>7b</sup> Monolayer films of PS<sub>50000</sub>-*b*-P4VP<sub>13000</sub> micelles were immersed in 50 mM HAuCl<sub>4</sub> aq. for 10 min at 20 °C, rinsed with water, and dried with nitrogen. This Au<sup>3+</sup>-doped film was placed in a vacuum chamber evacuated to  $1.2 \times 10^3$  Pa by a rotary pump and exposed to excimer VUV radiation ( $\lambda = 172$  nm) for 15 min. AFM images showed that individual AuNPs formed 3.0-nm high hemispherical bumps with an apparent diameter of 37.5 nm (not corrected for tip convolution).
  - Y. Yoneda, *Phys. Rev.* **1963**, *131*, 2010.